

28 Gb/s direct modulation heterogeneously integrated C-band InP/SOI DFB laser

Amin Abbasi,^{1,*} Jochem Verbist,^{1,2} Joris Van Kerrebrouck,² Francois Lelarge,³ Guang-Hua Duan,³ Xin Yin,² Johan Bauwelinck,² Gunther Roelkens,¹ and Geert Morthier¹

¹Photonics Research Group, INTEC, Ghent University—IMEC, Sint-Pietersnieuwstraat 41, 9000 Ghent, Belgium

²Design Group, INTEC, Ghent University – iMinds – IMEC, 9000 Ghent, Belgium

³III-V lab, a joint lab of 'Alcatel-Lucent Bell Labs France', 'Thales Research and Technology' and 'CEA Leti', Campus Polytechnique, 1, Avenue A. Fresnel, 91767 Palaiseau cedex, France

*amin@intec.ugent.be

Abstract: We demonstrate direct modulation of a heterogeneously integrated C-band DFB laser on SOI at 28 Gb/s with a 2 dB extinction ratio. This is the highest direct modulation bitrate so far reported for a membrane laser coupled to an SOI waveguide. The laser operates single mode with 6 mW output power at 100 mA bias current. The 3 dB modulation bandwidth is 15 GHz. Transmission experiments using a 2 km non zero dispersion shifted single mode fiber were performed at 28 Gb/s bitrate using a 2⁷-1 NRZ-PRBS pattern resulting in a 1 dB power penalty.

©2015 Optical Society of America

OCIS codes: (140.3490) Lasers, distributed-feedback; (250.5960) Semiconductor lasers; (200.4650) Optical interconnects; (250.5300) Photonic integrated circuits.

References and links

1. D. Miller, "Device requirement for optical interconnects to Silicon chips," *Proc. IEEE* **97**(7), 1166–1185 (2009).
2. G. T. Reed, G. Mashanovich, F. Y. Gardes, and D. J. Thomson, "Silicon optical modulators," *Nat. Photonics* **4**(8), 518–526 (2010).
3. S. Selvaraja, W. Bogaerts, P. Dumon, D. Van Thourhout, and R. Baets, "Subnanometer linewidth uniformity in silicon nanophotonic waveguide devices using CMOS fabrication technology," *IEEE J. Sel. Top. Quantum Electron.* **16**(1), 316–324 (2010).
4. Y. T. Hu, M. Pantouvaki, S. Brems, I. Asselberghs, C. Huyghebaert, M. Geisler, C. Alessandri, R. Baets, P. Absil, D. Van Thourhout, and J. Van Campenhout, "Broadband 10Gb/s graphene electro-absorption modulator on silicon for chip-level optical interconnects," *IEEE Electron Devices Meeting (IEDM)*, San Francisco, CA, Dec. (2014).
5. D. Feng, S. Liao, H. Liang, J. Fong, B. Bijlani, R. Shafiiha, B. J. Luff, Y. Luo, J. Cunningham, A. V. Krishnamoorthy, and M. Asghari, "High speed GeSi electro-absorption modulator at 1550 nm wavelength on SOI waveguide," *Opt. Express* **20**(20), 22224–22232 (2012).
6. L. Vivien, J. Osmond, J. M. Fédéli, D. Marris-Morini, P. Crozat, J. F. Damlencourt, E. Cassan, Y. Lecunff, and S. Laval, "42 GHz p.i.n Germanium photodetector integrated in a silicon-on-insulator waveguide," *Opt. Express* **17**(8), 6252–6257 (2009).
7. M. J. R. Heck, J. F. Bauters, M. L. Davenport, J. K. Doylend, S. Jain, G. Kurczveil, S. Srinivasan, Y. Tang, and J. E. Bowers, "Hybrid silicon photonic integrated circuit technology," *IEEE J. Sel. Top. Quantum Electron.* **19**(4), 6100117 (2013).
8. S. R. Jain, M. N. Sysak, G. Kurczveil, and J. E. Bowers, "Integrated hybrid silicon DFB laser-EAM array using quantum well intermixing," *Opt. Express* **19**(14), 13692–13699 (2011).
9. S. Keyvaninia, S. Verstuyft, L. Van Landschoot, F. Lelarge, G.-H. Duan, S. Messaoudene, J. M. Fedeli, T. De Vries, B. Smalbrugge, E. J. Geluk, J. Bolk, M. Smit, G. Morthier, D. Van Thourhout, and G. Roelkens, "Heterogeneously integrated III-V/silicon distributed feedback lasers," *Opt. Lett.* **38**(24), 5434–5437 (2013).
10. A. W. Fang, E. Lively, Y. H. Kuo, D. Liang, and J. E. Bowers, "A distributed feedback silicon evanescent laser," *Opt. Express* **16**(7), 4413–4419 (2008).
11. R. S. Tucker, "Green optical communications-part I: energy limitations in transport," *IEEE J. Sel. Top. Quantum Electron.* **17**(2), 245–260 (2011).
12. M. Asghari and A. V. Krishnamoorthy, "Silicon photonics: Energy-efficient communication," *Nat. Photonics* **5**(5), 268–270 (2011).
13. C. Kachris, K. Kanonakis, I. Tomkos, "Optical interconnection networks in data centers: recent trends and future challenges," *IEEE Communication Magazine*, Sept. 2013, 39 (2013).
14. G. Sakaino, T. Takiguchi, H. Sakuma, C. Watatani, T. Nagira, D. Suzuki, T. Aoyagi, and T. Ishikawa, "25.8 Gbps direct modulation of BH AlGaInAs DFB lasers with p-InP substrate for low driving current," in *Proc. International Semiconductor Laser Conf. (ISLC)*, Sep. 2010, 197–198, ThB5.

15. N. Nakamura, M. Shimada, G. Sakaino, T. Nagira, H. Yamaguchi, Y. Okunuki, A. Sugitatsu, and M. Takemi, "25.8Gbps direct modulation AlGaInAs DFB lasers of low power consumption and wide temperature range operation for data center," in *Optical Fiber Communication Conference*, paper W2A.53 (2015).
16. S. Matsuo, T. Fujii, K. Hasebe, K. Takeda, T. Sato, and T. Kakitsuka, "Directly modulated buried heterostructure DFB laser on SiO₂/Si substrate fabricated by regrowth of InP using bonded active layer," *Opt. Express* **22**(10), 12139–12147 (2014).
17. C. Zhang, S. Srinivasan, Y. Tang, M. J. R. Heck, M. L. Davenport, and J. E. Bowers, "Low threshold and high speed short cavity distributed feedback hybrid silicon lasers," *Opt. Express* **22**(9), 10202–10209 (2014).
18. G. de Valicourt, G. Levaufre, Y. Pointurier, A. Le Liepvre, J.-C. Antona, C. Jany, A. Accard, F. Lelarge, D. Make, and G.-H. Duan, "Direct Modulation of Hybrid-Integrated InP/Si Transmitters for Short and Long Reach Access Network," *J. Lightwave Technol.* **33**(8), 1608–1616 (2015).
19. S. Keyvaninia, M. Muneeb, S. Stanković, P. J. Van Veldhoven, D. Van Thourhout, and G. Roelkens, "Ultra-thin DVS-BCB adhesive bonding of III-V wafers, dies and multiple dies to a patterned silicon-on-insulator substrate," *Opt. Mater. Express* **3**(1), 35–46 (2013).
20. J. S. Gustavsson, A. Haglund, J. Bengtsson, and A. Larsson, "High-speed digital modulation characteristics of oxide-confined vertical-cavity surface-emitting lasers—numerical simulations consistent with experimental results," *IEEE J. Quantum Electron.* **38**(8), 1089–1096 (2002).
21. H. Zhu, Y. Xia, and J.-J. He, "Pattern dependence in high-speed Q-modulated distributed feedback laser," *Opt. Express* **23**(9), 11887–11897 (2015).
22. A. Chiuchiarelli, M. J. Fice, E. Ciaramella, and A. J. Seeds, "Effective homodyne optical phase locking to PSK signal by means of 8b10b line coding," *Opt. Express* **19**(3), 1707–1712 (2011).

1. Introduction

Silicon photonics is emerging as the platform of choice for the integration of photonics with electronic integrated circuits. Its compatibility with CMOS fabrication technology as well as the possibility to implement very compact optical circuits makes it an important candidate for the implementation of low-cost and high-speed transceivers [1,2]. State-of-the-art passive waveguide circuits are available on this platform and are accessible through multi-project wafer services [3]. The integration of high performance active components like modulators [1,4,5], photodiodes [6] and lasers [7–10] is an intensive field of research. Levering photonics for the data transmission and processing will improve speed and power consumption in interconnectors especially in the short links [11–13]. The workhorse of such interconnectors is the optical modulator.

Direct modulation of laser diodes for high-speed transceivers has significant advantages over the use of external modulators in terms of power consumption, fabrication complexity and compactness [14–18], especially for short distance optical interconnects. As has been discussed in [1,2], MZ based modulators require a long interaction length (~mm's) if a low drive voltage is desired. They also suffer from substantial insertion loss, which implies using a higher power laser source to compensate for the losses. High performance directly modulated lasers on an InP platform and bonded to a silicon substrate have been demonstrated recently [14–16]. Given the mentioned advantages of silicon photonics it would be desirable to have directly modulated transmitters with a high modulation bandwidth coupled to a silicon photonic integrated circuit. Heterogeneous integration is an attractive approach to realize this, as it is scalable to large arrays of devices [7].

So far however, only few results on the high speed direct modulation capabilities of heterogeneously integrated laser diodes have been published. In [17], a hybrid DFB laser was directly modulated at 12.5 Gb/s with an extinction ratio of 2.8 dB for a 1.5 V voltage swing. In [18], a much higher bitrate of 21.4 Gb/s is demonstrated using a heterogeneously integrated tunable laser, using an external cavity resonance (photon-photon resonance). However, the use of an external cavity resonance requires fine-tuning. Therefore it complicates the control of the laser diodes and increases the power consumption.

This paper reports on the high speed direct modulation of DFB membrane lasers, heterogeneously integrated on and coupled to a SOI waveguide circuit. 28 Gb/s NRZ modulation with 2 dB extinction ratio is demonstrated. After transmission over 2 km of dispersion shifted single mode fiber, we incur only 1 dB power penalty. The laser is single mode and has 6 mW single facet output power at 100 mA bias.

2. Laser structure and fabrication

The laser structure is shown in Fig. 1(a). It consists of a III-V gain section that is integrated on top of a silicon-on-insulator waveguide circuit by means of adhesive bonding using DVS-BCB [19]. 400 nm thick Si waveguide structures are used for an efficient coupling between the III-V mesa and the Si rib waveguide by adiabatic taper structures [9]. DFB gratings are patterned on the 400 nm Si rib waveguides using deep UV lithography and are 180 nm etched. The DFB grating period is 245 nm and has 50% duty cycle. More details on the III-V processing can be found in [9]. GSG pads with a pitch of 100 μm are patterned for high-speed measurements. The DFB laser's length is 340 μm and two tapers of 220 μm long are used to realize an efficient and low reflection coupling from the laser to the silicon waveguide.

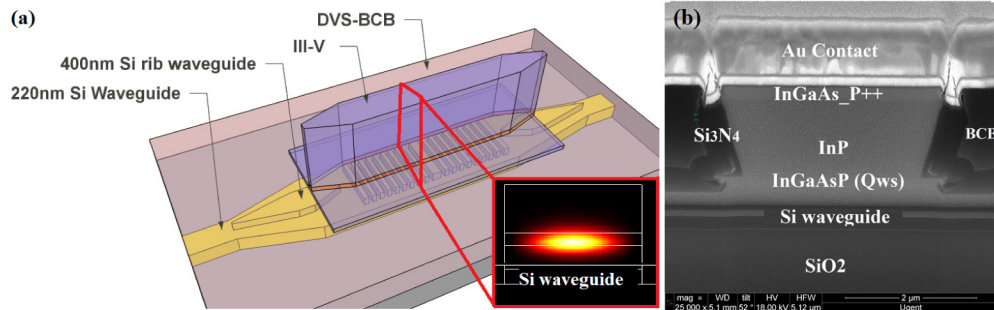


Fig. 1. (a) Schematic of the realized device with the lasing mode intensity profile, predominantly confined in the III-V waveguide; (b) cross section of the fabricated hybrid DFB laser

A cross section of the fabricated device is shown in Fig. 1(b). The III-V epitaxial layer stack that is used, consists of a 200 nm thick n-InP contact layer, two 100 nm thick InGaAsP separate confinement heterostructure layers (bandgap wavelength 1.17 μm), 6 InGaAsP quantum wells (6 nm thick, emission wavelength 1.55 μm) surrounded by InGaAsP barriers, a 1.5 μm thick p-InP top cladding and a 300 nm p + + InGaAs contact layer. A V-shaped mesa structure, realized by wet etching, allows achieving a high confinement factor in the active section and to realize sharp taper tips. The confinement factor in the 6 quantum wells is calculated to be 12%. The passivation stack of PECVD Si_3N_4 and DVS-BCB reduces the parasitic capacitance of the device and creates an effective electrical isolation.

3. Static characteristics

The laser static characteristics were measured using a Keithley 2400 current source and two DC probes. Light was coupled to a single mode fiber from the Si waveguide by a grating coupler with a 7 dB fiber-to-chip coupling loss. The measurements were done on a temperature-controlled stage at 20 $^\circ\text{C}$. The laser optical spectrum and the L-I-V curve are depicted in Fig. 2. The SMSR is more than 45 dB. The laser threshold current I_{th} is 17 mA and a waveguide coupled optical output power of 6 mW is obtained at a drive current of 100 mA. The kink in the L-I curve is attributed to a mode hop from the shorter wavelength band edge mode of the DFB laser to the longer wavelength mode due to device heating (an effect which only occurs in CW operation and not under dynamic operation). The extracted coupling coefficient from the stop-band of the laser spectrum in the low gain approximation is about 135 cm^{-1} . This corresponds with a DVS-BCB bonding layer thickness of 50 nm. The limited slope efficiency of the device is attributed to scattering losses and incomplete pumping of the taper sections. Note that the current plotted in Fig. 2(b) represents both the current injected in the DFB laser and taper structures and that the output power is the single facet output power of the symmetrical DFB laser. The series resistance of the device is 10 Ω . The laser operates at 1566 nm, which is close to the gain peak of the laser structure.

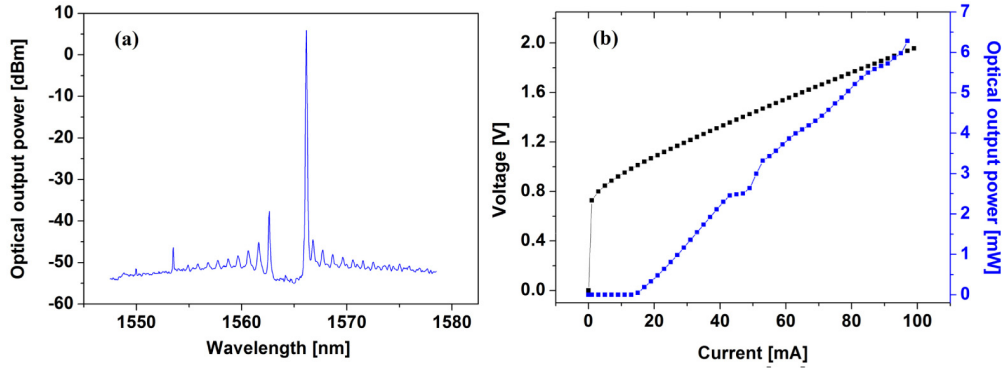


Fig. 2. a) DFB spectrum and b) LIV curve of the device (waveguide-coupled single facet output power).

4. Dynamic characteristics

Small signal modulation measurements were done using a Keysight PNA-X 67 GHz network analyzer. The RF signal was combined with a DC bias current using a bias-tee, and a GSG high speed probe with a 100 μm pitch was used to apply the combined signal to the DFB laser. The small signal response of the device is presented in Fig. 3(a) for different bias currents. At 100 mA bias current the 3 dB bandwidth is 15 GHz. The resonance frequency as a function of $(I-I_{\text{th}})^{1/2}$ is shown in Fig. 3(b). The higher modulation bandwidth of this laser in comparison with other demonstrated hybrid lasers is attributed to the small laser mode volume and high confinement factor in the active region.

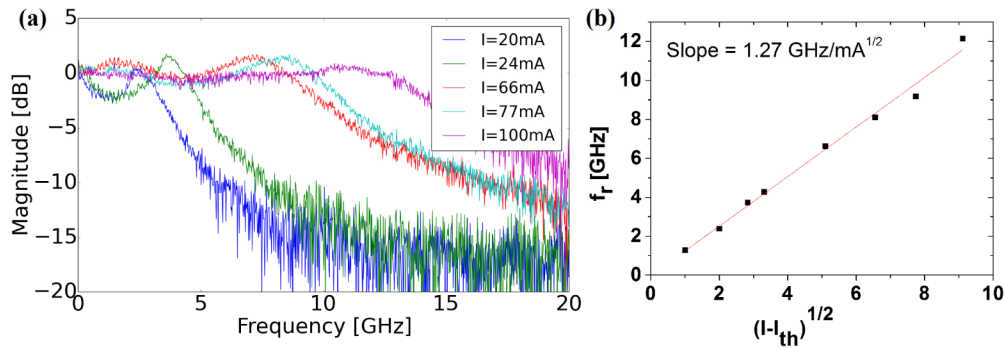


Fig. 3. (a) Small signal response at different bias currents, (b) the dependence of relaxation oscillation frequency (f_r) on the driving current.

For the large signal modulation measurements a SHF 12100B pulse pattern generator (PPG) was used for variable bitrate measurements with adjustable pattern lengths. The output of the PPG was amplified by a SHF S807 broadband RF amplifier. An RF-voltage of 2 V_{pp} (assuming 50 Ω load) was applied to the laser to realize its large signal modulations. As the laser is not 50 Ω terminated a much lower voltage swing ($<1\text{V}$) on the laser is expected. Eye diagrams were measured using a Tektronix DSA 8300 sampling oscilloscope. Eye diagrams as a function of modulation rate, measured using a 40 GHz pin photodiode with external TIA, are shown in Fig. 4 (back-to-back).

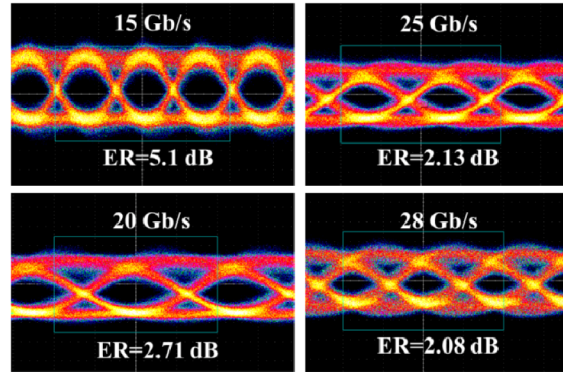


Fig. 4. Eye diagrams for back-to-back operation at 15, 20, 25 and 28 Gb/s using a 2^7-1 pattern length (bias current of 100 mA at 20°C).

At 20 and 25 Gb/s modulation speed, the bit error rate (BER) measurements were done both back-to-back and using 1 km standard single mode fiber (SSMF) using a 2^7-1 NRZ-PRBS pattern. The results are presented in Fig. 5.

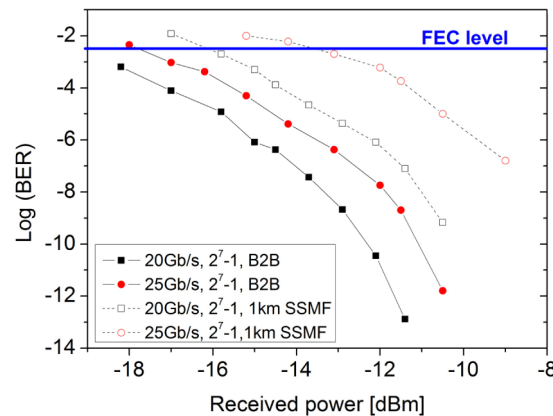


Fig. 5. BER measurements for back-to-back and 1 km single mode fiber configurations using a 2^7-1 NRZ-PRBS pattern (bias current of 100 mA at 20°C).

As shown in Fig. 5, assuming 7% hard-decision (HD) forward error correction (FEC), 2.4 dB and 4.0 dB power penalties were measured, for 20Gb/s and 25Gb/s transmission over 1 km SMF respectively. At a bit error rate of 10^{-9} a power penalty of 2 dB is obtained at 20 Gb/s. Back-to-back measurements and transmission measurements using a 2 km non zero dispersion shifted single mode fiber (NZ_DSSMF) were carried out at 28 Gb/s at a bias current of 100 mA at 20°C. A Sumitomo photodiode with a packaged limiting transimpedance amplifier was used at the receiver side. The eye diagrams back-to-back and after the 2 km NZ_DSSMF are shown in Fig. 6. There is little impact on the eye opening after the 2 km NZ_DSSMF. BER measurements were realized to verify the data transmission quality at 28 Gb/s for different PRBS pattern lengths (see Fig. 7). Less than 1 dB power penalty at a BER of 10^{-9} was measured using the 2 km NZ_DSSMF at 28 Gb/s using a data stream length of 2^7-1 . To the best of the authors' knowledge, this is the highest direct modulation speed for a membrane DFB laser heterogeneously integrated on and coupled to a SOI waveguide. Degradation can be observed for longer word length, as also observed and explained in other works [20,21]. No strong pattern dependence was observed at 10 or 15 Gb/s. Using encoding methods such as 8b/10b may be useful to reduce this pattern effect [22].

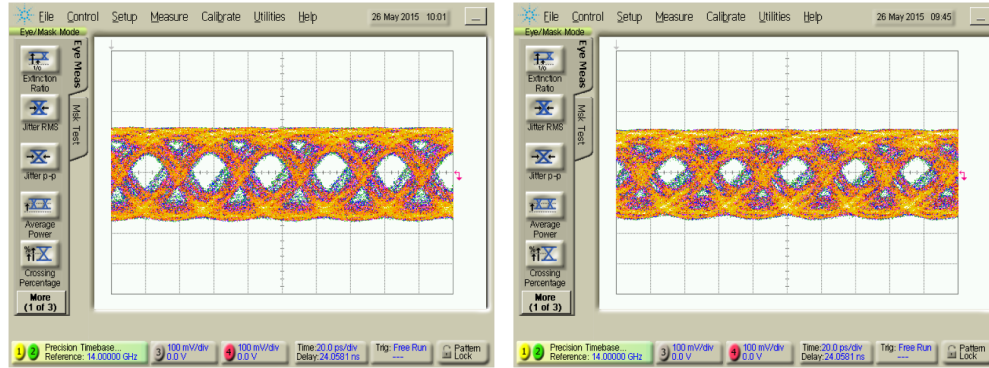


Fig. 6. Eye diagrams for back-to-back (left) and after 2 km NZ_DSSMF fiber transmission (right) at 28 Gb/s using a 2^{11} -1 data pattern length (bias current of 100 mA at 20°C).

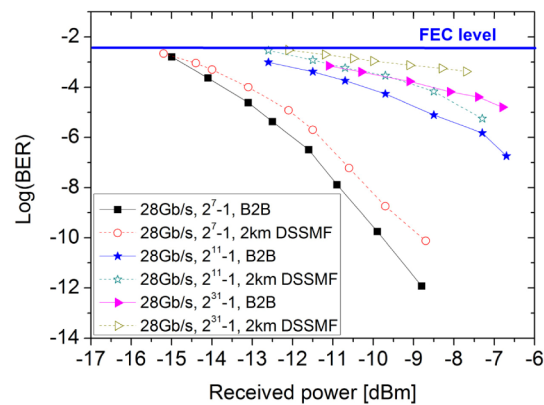


Fig. 7. 28 Gb/s BER measurements for back-to-back and 2 km NZ_DSSMF configurations (bias current 100 mA).

5. Conclusion

An InP-on-SOI heterogeneously integrated DFB laser for high-speed direct modulation has been realized. 28 Gb/s direct modulation with 2 dB extinction ratio was demonstrated in a back-to-back configuration. Transmission of 25 Gb/s data over a 1 km SSMF and of 28 Gb/s data over a 2 km NZ_DSSMF using 2^7 -1 NRZ-PRBS pattern was also demonstrated, with power penalties ranging from 4 dB to 1 dB. Further speed improvement can be realized by wavelength detuning from the gain peak, better cooling, an optimized device geometry (e.g. by electrically disconnecting the taper amplifiers from the DFB laser section and reducing the laser active area resulting in a lower RC time constant) and close integration with a proper low impedance laser driver chip. An impedance-matched design would allow the directly modulated laser to be driven by <1V CMOS IC, providing additional reduction in size, cost and power consumption of the transmitter. Using Al-containing quaternary materials in the active region, which have higher differential gain coefficient, could further improve the high-speed (as well as thermal) properties of the device. Further improvement in power consumption can be realized by shortening the laser cavity length [14, 17], implementing a high reflectivity mirror on one side of the DFB laser and again by implementing passive III-V taper structures that don't need to be electrically pumped. These devices enable the realization of 4x28 GbE wavelength division multiplexed or parallel optics transceivers.

Acknowledgment

The authors acknowledge the Belgian IAP network Photonics@be 14/GOA/034 and the UGent special research fund BOF for their support.